Available online at www.sciencedirect.com
ScienceDirect
Journal of Power Sources 179 (2008) 121–131
JOURNAL OF POWER SOURCES
www.elsevier.com/locate/jpowsour

Particle swarm optimization applied to the co-design of a fuel cell air circuit

Ali Sari, Christophe Espanet, Daniel Hissel *

University of Franche-Comté, FEMTO-ST Laboratory, ENISYS Department, FCLAB, Rue Thierry Mieg, 90010 Belfort Cedex, France

Received 27 August 2007; received in revised form 20 December 2007; accepted 1 January 2008
Available online 17 January 2008

Abstract

This paper presents an optimization approach applied to a whole fuel cell (FC) air supply system including its geometry and its control. The aim is to optimize its power consumption along with its mass. Particle swarm optimization (PSO) algorithm is used to define the design parameters of both permanent magnet synchronous motor (PMSM) and a fuzzy logic controller (FLC). The results are compared with those obtained by a sequential optimization process and advantages of co-design optimization approach are clearly shown. Indeed, a significant reduction of the objective function (made up on both motor mass and energy consumption) on a considered operating cycle can be obtained.

Keywords: PSO; Fuzzy logic controller; Permanent magnet synchronous motor; Co-design; Fuel cell air circuit

1. Introduction

Since 90s, problems of the greenhouse gas emissions control and hydrocarbon energy resources exhaustion, started again researches on fuel cell (FC) in many fields, such as transport, stationary power generation and portable applications [1]. Among these fields, the surface transports, that strongly use oil-based hydrocarbons, is one of the sectors generating the strongest greenhouse gas emissions. On the opposite, a FC directly supplied by hydrogen does not generate locally any environmental pollution. From this point of view, it is an interesting alternative to the internal combustion engine.

A proton exchange membrane FC, which is the most commonly used FC in the transport area, is an electrochemical converter which delivers electrical power and thermal energy by a redox reaction starting from a fuel (generally hydrogen). The energetic efficiency of FC itself is relatively high compared to other more conventional technologies (#60% for proton exchange membrane fuel cell efficiency and #32% for internal combustion engine efficiency). But its output power decreases due to ancillary circuits (fuel (hydrogen) and fuel oxidizer (oxygen) supply, humidification, cooling, electric converter,. . .) that are necessary to the correct operation of the FC (Fig. 1). Among these ancillaries, the air supply circuit (oxygen) of the FC generator is particularly "greedy" in energy [2]. It is classically carried out by a motor-compressor. Electrical conversion net efficiency of the energy brought by the fuel is around 50% but up to 35% of the produced electrical energy is consumed by the ancillaries (among this part, the 2/3 are consumed by the air supply). Thus, air supply system optimization is an important milestone on the road of efficient FC systems [3]. In this context, the main goal of this paper is to propose a new methodological optimization approach. In manners of electrical engineering, the classical approach is to use sequential optimization. In this case, the design process has several steps starting from system geometry optimization to finish with the calculation of the control laws. Such a methodology has already been proposed in several papers. In [4] the driving engine design of the compressor unit is proposed. Similar works are carried out on other engines in [5,6]. [2] deals with an optimization of the air supply circuit controller to improve system performances. More generally, controller optimization for many engines are carried out in [7,8]. In [9], actuator control optimization is performed based only on the optimization of the scaling factors of a FLC. In [10], PSO is used to define parameters of a PID controller in order to improve its performances. But is it really the optimal system

* Corresponding author. Tel.: +33 384 58 36 21; fax: +33 384 58 36 36.
E-mail addresses: ali.sari@edu.univ-fcomte.fr (A. Sari), christophe.espanet@univ-fcomte.fr (C. Espanet), daniel.hissel@univ-fcomte.fr (D. Hissel).

0378-7753/$ – see front matter © 2008 Elsevier B.V. All rights reserved.
doi:10.1016/j.jpowsour.2008.01.018

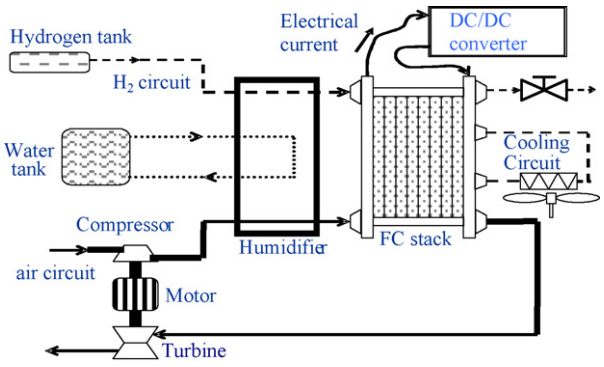

Fig. 1. Basic schema of a fuel cell system [4].

that is obtained with all these sequential methodologies? Our proposal is to compare this classical approach to a simultaneous optimization (i.e. optimization of the whole system at the same time) methodology. Such an approach has been presented in [11,12] concerning mechanics, electronics and micromachine domain and is similar to a multi-objective optimization [13]. The co-design being an emergent idea in electrical engineering, the references are still limited. Our aim will thus be to apply a co-design approach in order to evaluate its effectiveness and to compare it with the sequential one.

The paper is organized as follows. In Section 2, an overview of the driving motor and compression head modelling is presented and fuzzy logic controller is introduced. Section 3 presents particle swarm optimization (PSO) and its implementation on the considered co-design problem. The results obtained by both optimization methodologies (sequential and simultaneous) are compared in Section 4. Finally, Section 5 concludes this paper by pointing the key results and the possible outlooks.

2. Air supply circuit modelling and control

The considered air supply subsystem is here a motor-compressor built up from a rotary compressor and from a permanent magnet synchronous motor, which enables, associated to efficient control laws, to supply the FC stack with the air flow, in order to produce the desired electrical power [14]. In case of use with a 5 kW proton exchange membrane fuel cell, considered specifications for this system are the following:

- Maximum mass flow: 10 g s^{-1},
- Maximum absolute outlet pressure: 2 bars,
- Rated rotational speed: 3000 rpm,
- Nominal mass flow: 6 g s^{-1}.

2.1. Analytical model of PMSM in rotor reference frame

Recent developments in microprocessors, magnetic materials and semiconductors technologies have offered an excellent opportunity to use ac motors in high performance drive systems. PMSM became at the top of ac motors in the medium range of power and it became a very common choice in driving technology over the last few years due to some of its inherent advantages. Those include high torque to current ratio, large power to weight ratio, high efficiency and robustness.

PMSM is modelled with an equivalent Park machine which makes it possible to simplify motor equations. Inputs of this model are the three phase voltages (v_a, v_b, v_c) coming from the inverter. Thanks to Park transformation, forward and quadratic voltages (v_d, v_q) can be obtained from these three voltages. Motor flux expressions on forward and quadratic axes make it possible to evaluate forward and quadratic currents (i_d, i_q).

$$\begin{bmatrix} v_d \\ v_q \end{bmatrix} = R_s \begin{bmatrix} i_d \\ i_q \end{bmatrix} + \frac{d}{dt}\begin{bmatrix} \psi d \\ \psi q \end{bmatrix} + \theta^* P\left(\frac{\pi}{2}\right)\begin{bmatrix} \psi d \\ \psi q \end{bmatrix}, \quad (1)$$

$$\begin{bmatrix} v_d \\ v_q \end{bmatrix} = R_s \begin{bmatrix} i_d \\ i_q \end{bmatrix} + \frac{d}{dt}\begin{bmatrix} \psi d \\ \psi q \end{bmatrix} + \theta^*\begin{bmatrix} \psi d \\ \psi q \end{bmatrix}, \quad (2)$$

where

$$\psi d = (L_d + l'_d)i_d + \sqrt{\frac{3}{2}}\psi_f, \quad (3)$$

$$\psi q = (L_q + l'_q)i_q. \quad (4)$$

L_d and L_q are the forward and quadratic axes cyclic inductances and l'_d and l'_q the forward and quadratic axes leakage inductances.

Expression of the motor electromagnetic torque (T_m) can thus be obtained:

$$T_m = pi_q\left(((L_d + l'_d) - (l_q + l'_q))i_d - \sqrt{\frac{3}{2}}\psi_f\right). \quad (5)$$

With p the number of poles and ψ_f the magnetisation flux per pole.

Then the variables such as ψ_f, e (electro-motive force), L_d, L_q, m (mutual between two phases of machine) and the torque can be expressed with motor structural parameters and a completely adjustable model of the motor is obtained.

In our case, 11 parameters defining the PMSM structure are considered. These parameters are:

$$\begin{cases} R_{ecs}(\text{stator yoke external ray}) = 61.6\,\text{mm} \\ h_{cs}(\text{stator yoke height}) = 5.9\,\text{mm} \\ h_d(\text{cog height}) = 17.7\,\text{mm} \\ l_d(\text{cog width}) = 5\,\text{mm} \\ \text{ent(air–gap)} = 1\,\text{mm} \\ h_{ai}(\text{magnet height}) = 3\,\text{mm} \\ h_{cr}(\text{rotor yoke height}) = 6.1\,\text{mm} \\ L_{fer}(\text{machine length}) = 30\,\text{mm} \\ p(\text{pole pair number}) = 2 \\ d_{fil}(\text{wire diameter}) = 1.94\,\text{mm} \\ \text{ns(windings number of turns)} = 40 \\ R_s(\text{stator coil resistance}) = 0.17\,\Omega \\ L_s(\text{stator coil inductance}) = 6.83.10^{-4}\,\text{H} \end{cases}$$

Numerical values are the ones corresponding to the starting values that have been used next in the design process.

2.2. Analytical model of compressor

Rotary vane compressor model is constituted of four inputs (rotational speed, inlet air temperature, and inlet and outlet air pressures) and four outputs (air mass flow, air outlet temperature, compressor torque and mechanical power). Parameters used for modelling are the compressed volume per revolution ($V_{comp/rev}$) obtained thanks to the compressor sizes, air heat capacity (c_p) and air mass constant (r_{air}).

The expression of air mass flow (q_m) is depending on rotational speed (ω) of compressor according to

$$q_m = \frac{1}{2\pi}\eta v V_{comp/rev}\omega\rho_{air} \quad (6)$$

with ω: rated rotational speed (rpm), ρ_{air}: air inlet density (kg m^{-3}), q_m: mass flow (kg s^{-1}), $V_{comp/rev}$: volume compressed by revolution (m^3 rev^{-1}), ηv: volumetric efficiency of rotary vane compressor.

Other important relation for compressor modelling is the expression of requested power linked to air flow and pressure ratio. This relation is obtained from the temporal derivative of the work capacity needed to compress the air value from the inlet to the outlet pressure.

$$P_c = \frac{1}{\eta_{ad}\eta_m} q_m c_p T_{incomp}\left[\left(\frac{p_{out}}{p_{in}}\right)^{(\gamma-1/\gamma)} - 1\right] \quad (7)$$

with p_{in} and p_{out}: inlet air pressure (Pa) and outlet air pressure (Pa), T_{incomp}: inlet air temperature (K), c_p: air heat capacity, η_{ad}: adiabatic efficiency of rotary vane compressor, η_m: mechanic efficiency of rotary vane compressor, γ: polytrophic coefficient which depends on compressor load conditions (friction and heat transfers).

Finally, compressor outlet pressure is defined by pressure drops inside FC stack itself. Experimentally, it can be verified that the pressure drops are directly linked to gases circulation speed by a coefficient value 69.3 [2]. Thus the following empirical evolution is considered here (for the chosen FC stack):

$$p_{out} = p_{in} + 69.3\omega \quad (8)$$

2.3. Design a fuzzy logic controller

Fuzzy systems are being used successfully in an increasing number of application areas, they use linguistic rules to describe systems. Fuzzy logic provides a general concept for description and measurement. Most fuzzy logic systems encode human reasoning into a program to make decisions or control a system. Fuzzy logic comprises fuzzy sets, which are a way of representing non-statistical uncertainty and approximate reasoning, which includes the operations, used to make inferences in fuzzy logic.

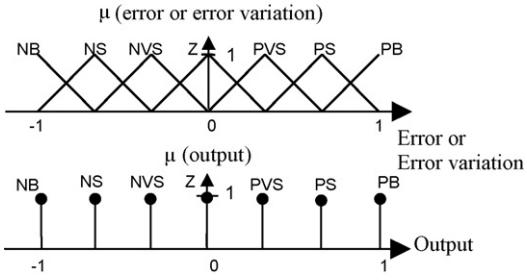

Fig. 2. Input and output membership function.

2.3.1. The fuzzy logic controller

The fuzzy control comprises three steps: fuzzification, inference, defuzzification [8]. In the first step, the FLC receives normalized physical size as input. The input is then developed in terms of a set of N membership functions (MF) which cover the range of interest of the corresponding indicator. Each MF is weighted according to its degree of membership m_i in the development. Typically, for real-time control triangular MFs are used for their simplicity (Fig. 2).

In the second step, the inference operation represents the if-then implication. The goal is to interconnect input membership and output membership of the controller. In the last step, defuzzification, the results of the inference step are combined into a single value for each controller output.

In the present case, for implementation of internal air flow regulator, Takagi-Sugeno fuzzy logic controllers have been used because they allow minimizing sampling time. In order to regulate and supply the required air quantity with an acceptable response time to the FC stacks, a non-linear fuzzy PD + I regulator (Fig. 3) has been chosen because of its high dynamic, precision and robustness [15].

2.3.2. FLC considered optimization parameters

In our case, the following tuning parameters of the controller are considered like most significant (Fig. 3):

- Three parameters corresponding to the scaling factors,
- Six parameters corresponding to the starting points and apex points of the membership functions,
- One parameter corresponding to the integral corrective coefficient.

Those are:

$$\begin{cases} PS_e(\text{positive small membership value on input entry of controller}) = 0.254 \\ PVS_e(\text{positive very small membership value on error input}) = 0.033 \\ PS_{de}(\text{positive small membership value on the error variation input}) = 0.7 \\ PVS_{de}(\text{positive very small membership value on the error variation}) = 0.21 \\ NS_s(\text{negative small membership value on the output}) = -0.8 \\ NVS_s(\text{negative very small membership value on the output}) = -0.615 \\ e_m(\text{scaling factor on the error input}) = 10\,\text{g s}^{-1} \\ de_m(\text{scaling factor on the error variation input}) = \dfrac{1}{\tau.T}(\tau + 0.4T)T_e e_m \\ g_m(\text{scaling factor on the output}) = \dfrac{2.07}{KT}(\tau + 0.4T)e_m \\ K_i(\text{coefficient of the integral correction}) = \dfrac{1.6}{KT} \end{cases}$$

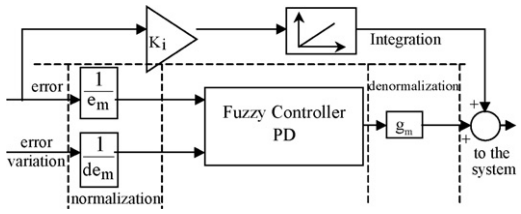

Fig. 3. Scheme of fuzzy PD + I controller principle.

with τ: time-constant, T: delay, K: static gain, T_e: sampling period.

3. Optimization

3.1. Considered operating cycle and objective function

The complete air supply circuit system is tested on a step set point and on a vehicle driving cycle. The first one presents an amplitude of $10\,g\,s^{-1}$ during a 138-ms cycle and the second one is a vehicle normalized mission profile (Fig. 4) that is deduced from the vehicle simulator program, Advisor® (profile "CYC_UDDS: Urban Dynamometer Driving Schedule"), used in embedded FC systems experimentation [16].

In order to optimize this system for these set points the objective function has to be defined. For example, objective function (f) is here, for step set point the following:

$$f = \frac{\text{rt}}{\text{rrt} \cdot 2} + \frac{\text{ec}}{\text{rec} \cdot 2} \tag{9}$$

with rt the rising time, rrt the reference system rising time, ec the energy consumption and rec the reference system energy consumption.

That allows obtaining a 50% influence of the energy criterion and a 50% influence of the rising time on the optimization, leading to both an economic and dynamic system.

3.2. The reference system

Classically, optimization methodologies applied to this kind of system are sequential, firstly optimizing the actuator alone,

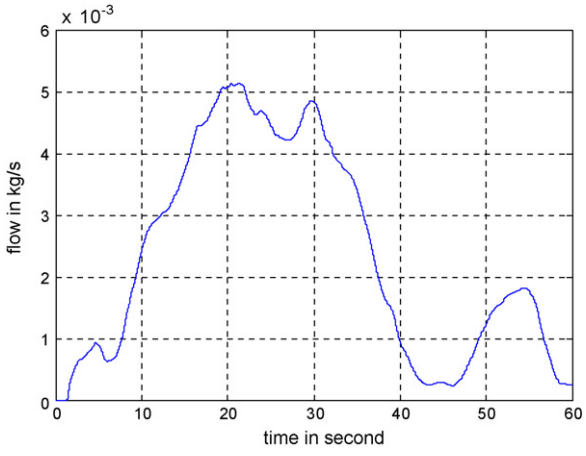

Fig. 4. Fuel cell air mass flow ($kg\,s^{-1}$) consumption profile deduced from Advisor® (CYC_UDDS) on 60 s.

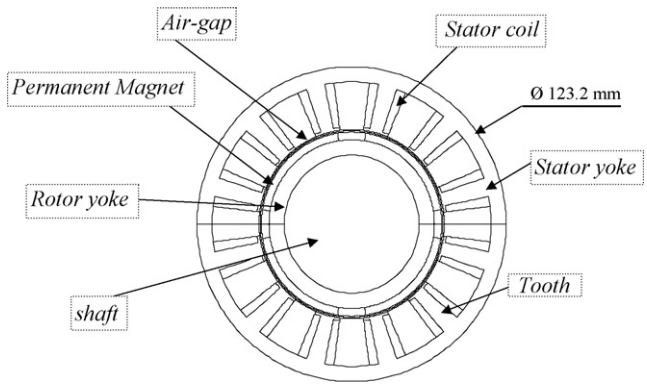

Fig. 5. The reference system PMSM structure.

then, defining the control for the actuator. Nevertheless, a limitation of this approach is that the capacities of the control are then limited by the actuator structure itself. The proposed new approach carries out system global optimization in calculating, jointly, both the optimal actuator structural parameters and the optimal control law parameters.

Thanks to the values of the reference system (given in previous section), the general shape of the motor (Fig. 5) and the control surface (Fig. 6), that reflects the control strategy imposed on the controller, can be obtained. This control surface gives a 3D representation of the control law realized by the FLC. The two first dimensions are the two normalized inputs of the FLC, the last dimension gives the normalized control output of the FLC. The reachable power greatly depends on the air flow within the stack. If the air supply circuit cannot respond quickly enough to the requested air flow, the FC life time is restricted. Thus, a chosen air flow dynamic (rise time: 138 ms) is here supposed to be requested by the FC. This rise time value has been obtained considering the oxygen volume (0.69 g) that is present inside the cathode compartment and the time during which this oxygen can supply the fuel cell in case of a nominal current set point on our real experimental 5 kW FC stack [17]. With this system, the air flow responses, obtained with the initial parameters settings, are plotted in Fig. 7 for step set point and Fig. 8 for a mission profile.

According to Fig. 7, the rising time is 125 ms and no steady static error is observed (for the reference system). The requirement of a rising time lower than 138 ms is respected. The system consumes 764 J for this cycle.

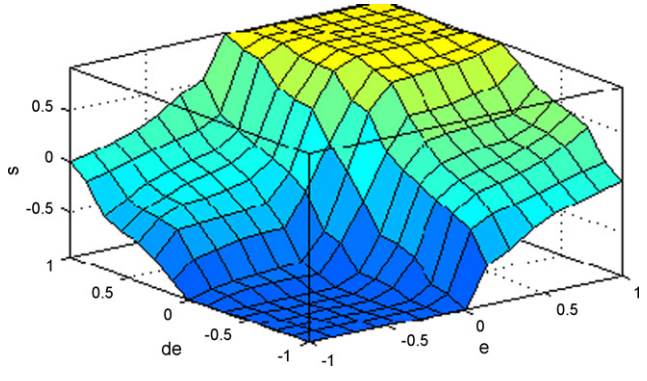

Fig. 6. The reference system control law strategy.

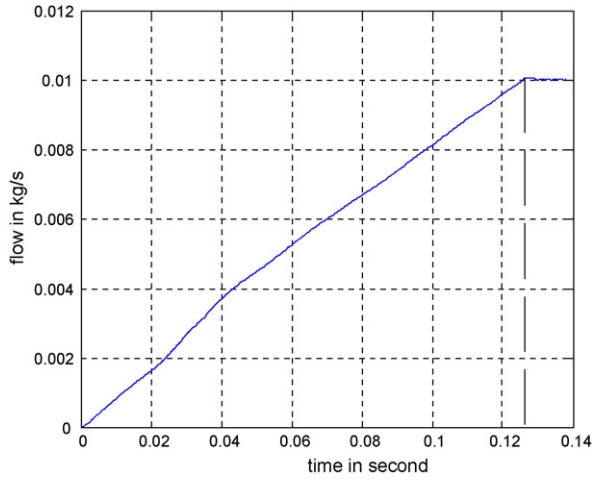

Fig. 7. The reference system response of air mass flow to step set point.

Fig. 8 gives the response of the system for dynamical solicitation. We can see that smearing errors is almost null (maximum transient error is about 8.17×10^{-4} g s^{-1}). The system consumes 45,129 J for this cycle of 60 s.

Now let us define the exploration domain for each optimization parameter.

$$\begin{cases} R_{ecs} \in [0.01, 0.1] \\ h_{cs} \in [0.003, 0.01] \\ h_{d} \in [0.005, 0.03] \\ l_{d} \in [0.003, 0.01] \\ \text{ent} \in [0.0005, 0.005] \\ h_{ai} \in [0.003, 0.01] \\ h_{cr} \in [0.003, 0.015] \\ L_{fer} \in [0.01, 0.1] \\ p \in [1, 6] \\ d_{fil} \in [0.0002, 0.005] \\ \text{ns} \in [0, 100] \end{cases} \quad \begin{cases} \text{PS}_{e} \in [0, 1] \\ \text{PVS}_{e} \in [0, 1] \\ \text{PS}_{de} \in [0, 1] \\ \text{PVS}_{de} \in [0, 1] \\ \text{NS}_{s} \in [-1, 0] \\ \text{NVS}_{s} \in [-1, 0] \\ \text{de} \in [0, 10] \\ g \in [0, 10] \\ k \in [0, 10] \end{cases} \tag{10}$$

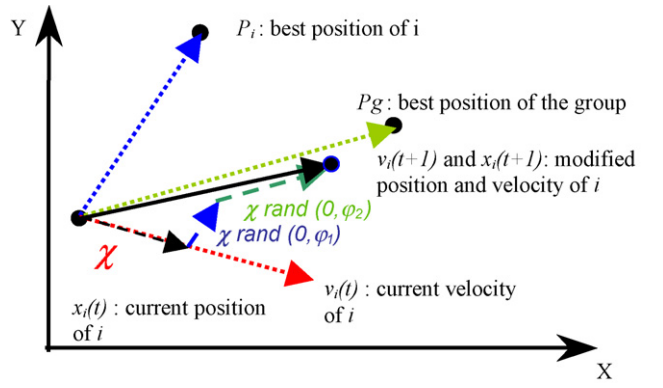

Fig. 9. Principle of the displacement of a particle in a two-dimensional space.

Exploration domain for each variable with R_{ecs}, h_{cs}, h_{d}, l_{d}, ent, h_{ai}, h_{cr}, L_{fer}, d_{fil} in millimeter.

3.3. Particle swarm optimization

3.3.1. Laws of the PSO

PSO belongs to the broad class of stochastic optimization algorithms. The ideas that underlie PSO are not inspired by the evolutionary mechanisms encountered in natural selection, but rather by the social behaviour of flocking organisms, such as swarms of honeybees and fish shoals. It has been observed that the behaviour of the individuals that belong to a flock adheres to fundamental rules like nearest-neighbour velocity matching and acceleration by distance [18,19]. PSO is a population-based algorithm that uses a population of individuals to probe promising regions of the search space. In this context, the population is called a swarm and the individuals are called particles. Each particle moves with an adaptable velocity within the search space (Fig. 9), and keep in its memory the best position it ever encountered. In the global variant of PSO, the best position ever reached by all individuals of the swarm is communicated to the whole particles. In the local variant, each particle is assigned to a neighbourhood consisting of a specified number of particles. In this

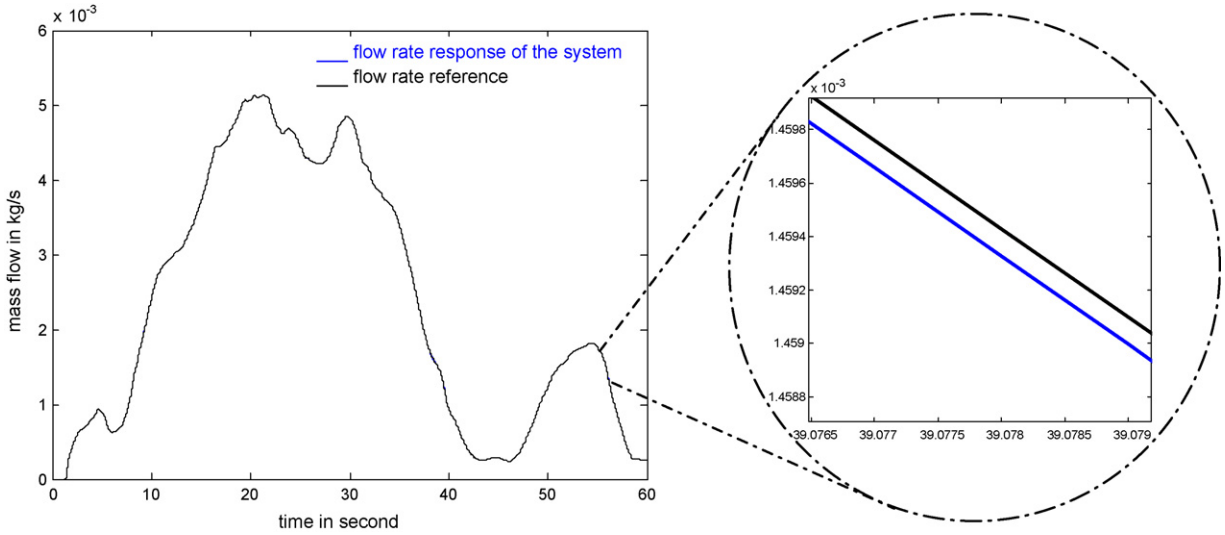

Fig. 8. The reference system response of air mass flow to step dynamic solicitation.

case, the best position ever reached by the particles that comprise the neighbourhood is communicated among them [20]. This paper considers the global variant of PSO only.

Let us assume a D-dimensional search space S, $S \subset \mathrm{IR}^D$, and a swarm consisting of N particles. The ith particle is a D-dimensional vector has the following coordinates:

$$X_i = (x_{i1}, x_{i2}, \ldots, X_{iD})^T \in S$$

The velocity of this particle is also a D-dimensional vector such as

$$V_i = (v_{i1}, v_{i2}, \ldots v_{iD})^T \in S$$

The best previous position encountered by the ith particle is a point in S, denoted as

$$P_i = (p_{i1}, p_{i2}, \ldots p_{iD})^T$$

If g is the index of the particle that reached the best previous position among all the individuals of the swarm, and t is the iteration counter. Then, according to the version of PSO, a parameter called the constriction factor is defined by Clerc [21]. The swarm is thus manipulated according to the following equations:

$$V_i(t+1) = \chi[V_i(t) + c_1 r_1(P_i(t) - X_i(t)) + c_2 r_2(P_g(t) - X_i(t))] \quad (11)$$

$$X_i(t+1) = X_i(t) + V_i(t+1) \quad (12)$$

where $i = 1, 2, \ldots, N$, χ is the constriction factor, c_1 and c_2 (with experimental value of 2.5) denote the cognitive and social parameters, respectively, and r_1, r_2 are random numbers uniformly distributed in the interval [0,1].

The value of the constriction factor is typically obtained through the formula [21]:

$$\left.\begin{aligned} \chi &= \frac{2\kappa}{\phi - 2 + \sqrt{\phi^2 - 4\phi}}, \quad \text{for } \phi > 4 \\ \chi &= \sqrt{\kappa}, \quad \text{for } \phi \le 4 \end{aligned}\right\} \text{with } \kappa = 1 \quad \text{and } \phi = c_1 r_1 + c_2 r_2 \quad (13)$$

3.4. Constraint handling

In the literature, several studies, which proposed to extend PSO to constrained optimization problems, are reported, and different constraint handling techniques were used.

Parsopoulus [22] converted the constrained optimization problem into a non-constrained optimization problem by adopting a non-stationary multi-stage assignment penalty function and then applying PSO to the converted problems. Ray [23] employed a Pareto ranking scheme to handle constraints, which is a concept of multi-objective optimization.

Here, a simple but efficient method is introduced to solve constrained optimization problems. The preserving feasibility strategy is implemented to deal with constraints. Two modifications of the PSO algorithms have been proposed:

(1) when updating the memories *pBest* (coordinates of best fitness value of each particles) and *gBest* (coordinates of best fitness value of all particles), each particle only keep feasible solutions in its memory and leave aside other solutions that do not respect imposed constraints,
(2) during the initialization process, one particle, at least, is initialized started with feasible solution.

Compared to other constraint handling techniques, this approach has the following advantages:

(1) It is quite simple. There is no pre-processing to take into account the constraints and there is neither complicated manipulation. Fitness function and constraints are handled separately, thus there are no limitations concerning the constraints.
(2) It is faster. The only part of the algorithm dealing with constraints is to check if a solution satisfies all the constraints. This will reduce the computation time when handling multiple or complicated constraints.

Examples of physical constraints are given as following:

- External radius of the rotor yoke < external radius of the magnets,
- Diameter of winding wire < spaces passage between two isthmuses of tooth,
- PSe > PVSe,
- PSde > PVSde, } Fuzzy logic parameters
- 35% >rate of filling of the notches …

3.4.1. Implementation of PSO

The implementation of PSO program is easy and only takes a few lines. For example, in our case, the algorithm programming on Matlab® uses 25 lines. More precisely the different steps of the PSO program are described in Fig. 10.

3.5. Optimization process

The control concept, using field oriented control and implementation of fuzzy logic controller on the motor-compressor group is shown in Fig. 11. Firstly, for this model, the PSO algorithm generates motor construction parameters and control law parameters. In the second step, the model is simulated. The third step consists in simulation result evaluation in order to calculate the value of optimization criterion f. Finally,

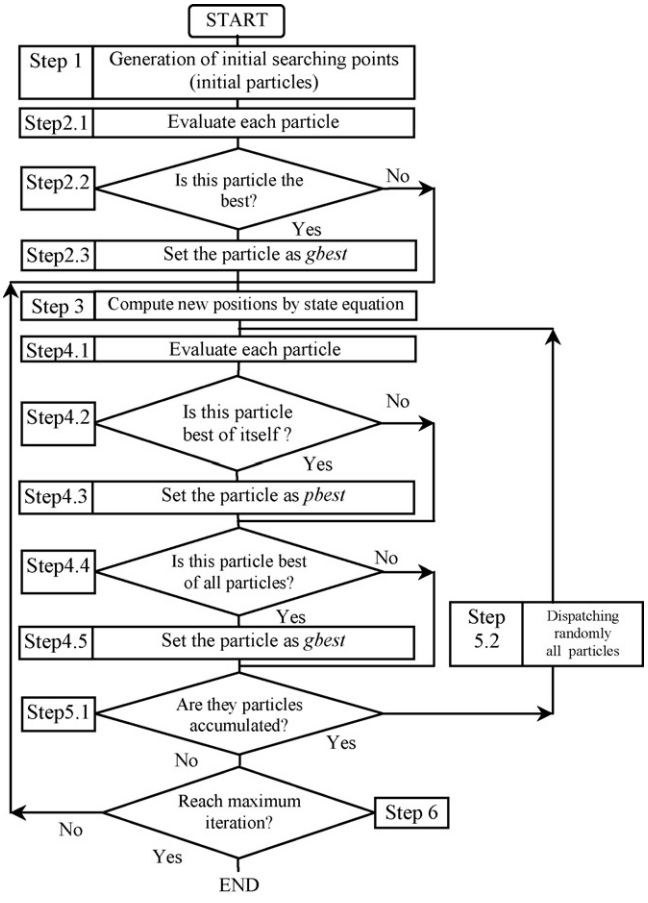

Fig. 10. Flow chart of optimization process by PSO.

a new set of optimization parameters is evaluated (cf. step 1).

In our case, all optimizations are based on 401 iterations and 20 particles in order to ensure equity in comparing the methods. According to numerous papers, the choice of 20 particles is suitable for a wide number of optimization processes. Stochastic optimization methods ensure finding the global optimum with an infinite time of optimization what is not really conceivable. The choice of 401 iterations is based on our own simulation know-how and on the constraint to have a reasonable computational time.

Let us have a look at the optimization progress (cf. Figs. 12 and 13). On Fig. 12, the progress (during iterations) of the state of particles is provided. The particles respecting all the imposed constraints are entered as good particles. We can observe the increase in the number of good particles with the

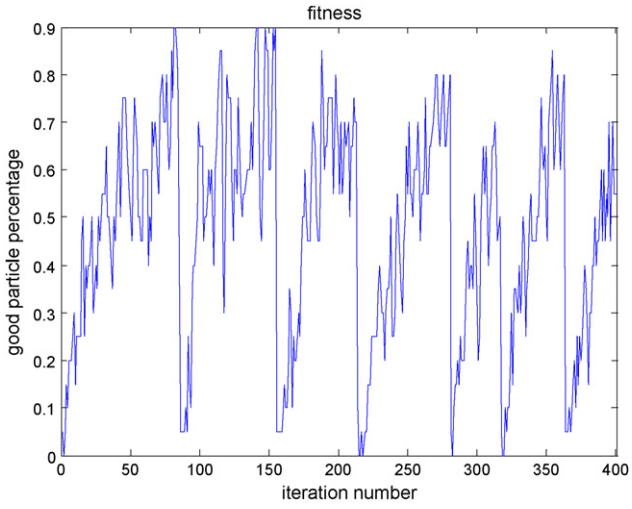

Fig. 12. Evolution of good particles percentage during optimization.

increase in the iteration count. Reaching a certain iteration count we see a sudden fall of the number of good particles which can be explained by the process of dispatching, i.e. when 90% of the particles are in an hypersphere dimension R (another variable), they are dispersed randomly in search space. That is a complementary function making it possible to decrease the probabilities of being blocked in a local minimum.

Fig. 13 provides the evolution of the objective function which begins with a value of 0.807 that corresponds to the objective function obtained for the reference system and stops with a value of 0.31 that is the value of the objective function obtained on the system defined by simultaneous optimization on an indicial solicitation. The objective function evolution becomes very slow after 250 iterations. Furthermore, particles are three times redistributed between iteration 250 and iteration 401. It is thus possible to say it is at least a local optimum.

4. Results

4.1. Sequential optimization

Firstly, a sequential optimization method for the motor-compressor and its control has been carried out. The optimization process starts with PMSM optimization based on an efficiency criterion. PSO leads to a PM motor with an efficiency of 95% (Fig. 14). Then using PSO, optimal control law parameters are computed (considering the two types of set points that have been considered). For instance, considering a step set

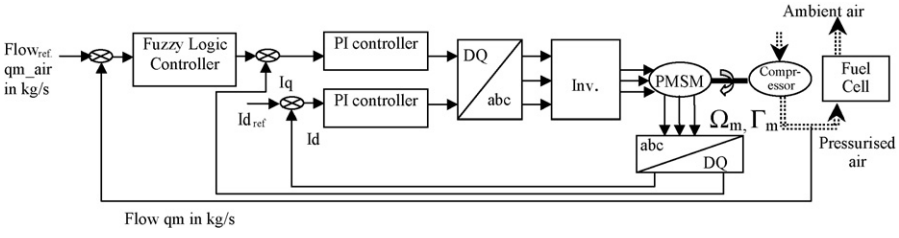

Fig. 11. System model.

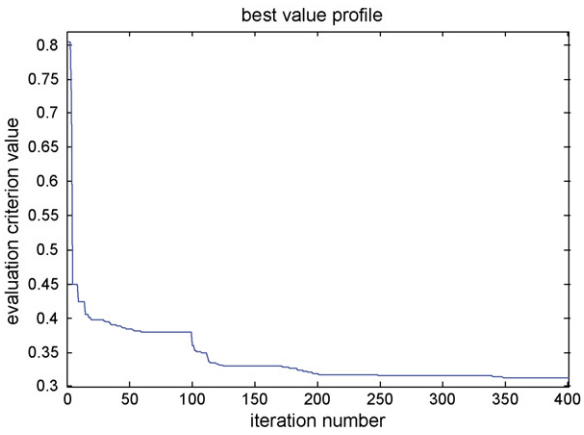

Fig. 13. Objective function evolution during optimization.

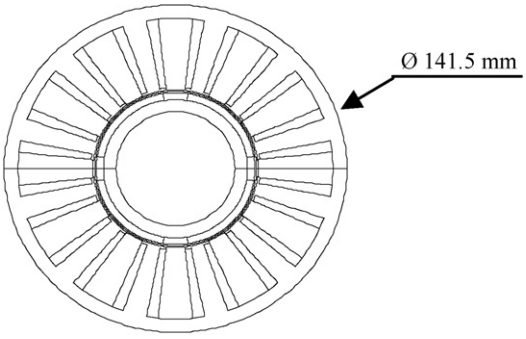

Fig. 14. PMSM structure (for indicial set point) for the system optimized by sequential method.

point, the control law obtained by PSO enable us to build the control surface presented in Fig. 15.

This motor-compressor group system provides a response in mass flow with a rising time of 132 ms, without steady-state error and with a consumption of 459 J for this cycle (Fig. 16).

Now, for the dynamic solicitation the control law obtained by PSO enables to build the control surface of Fig. 17. These control law and motor design provide a response in mass flow with very weak smearing errors corresponding to a maximal interval of 0.689 and a consumption of 9718 J on this 60 s cycle (Fig. 18).

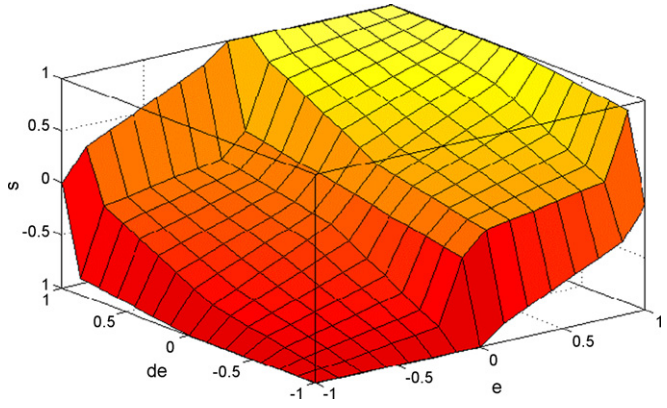

Fig. 15. Control law surface (for indicial set point) for the system optimized by sequential method.

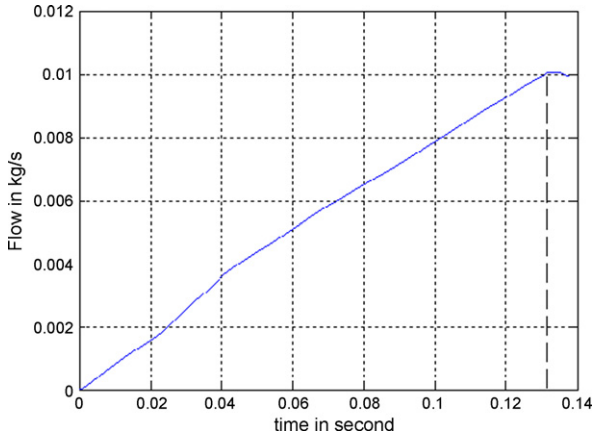

Fig. 16. Response in air mass flow at a step set point.

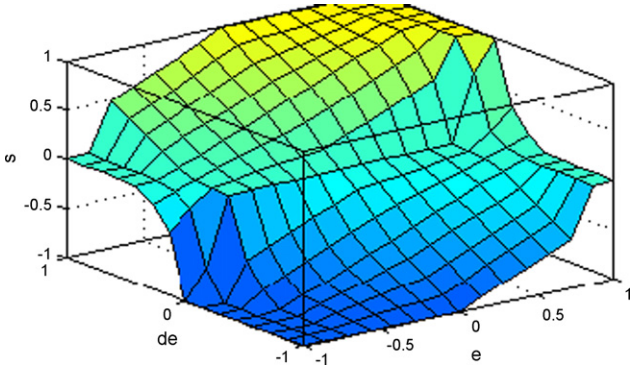

Fig. 17. Control surface obtained by sequential optimization.

4.2. Coupled optimization

Secondly, simultaneous optimization method for the motor-compressor and its control has been performed. Using this method, PSO carries out an iterative research in order to obtain the 21 parameters of the engine and the fuzzy controller parameters that will minimize the objective function. The objective function is defined to achieve the goals of desired consumption and performance.

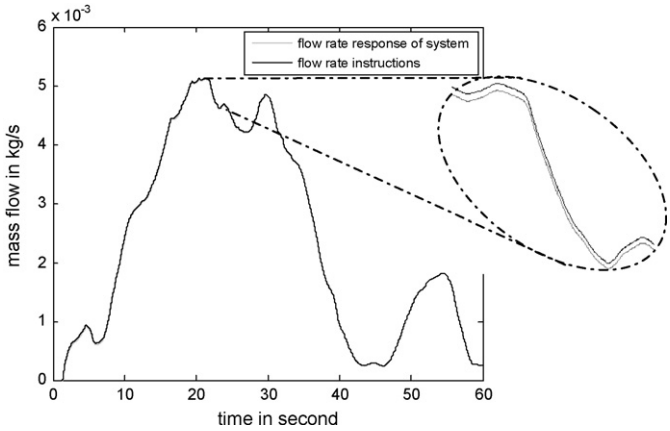

Fig. 18. Response in air mass flow for the dynamic set point.

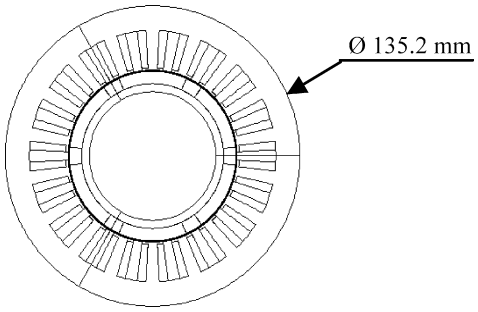

Fig. 19. PMSM structure for the system optimized simultaneously.

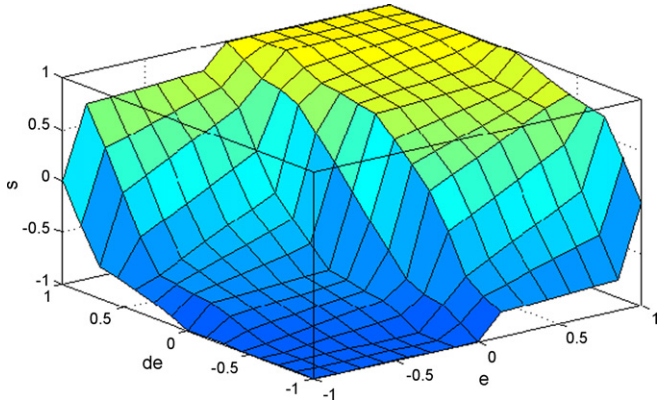

Fig. 20. Control law surface for the system optimized simultaneously.

For the step set point, the parameters obtained by PSO generate the motor geometry and the control surface shown in Figs. 19 and 20.

In this case, a rising time (for air mass flow) of 25 s and a steady-state error are obtained with a light over-shooting, and a consumption of 568 J. We can see the response in Fig. 21.

In short, we obtain, with a simultaneous optimization, a system much more powerful than the reference system or the system optimized sequentially and a system that has power consumption much lower than the reference one but a little energy-hungry than the sequentially optimized system.

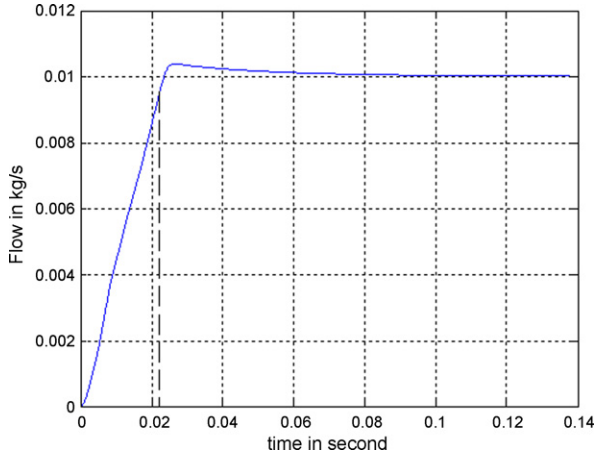

Fig. 21. Response in air mass flow step set point.

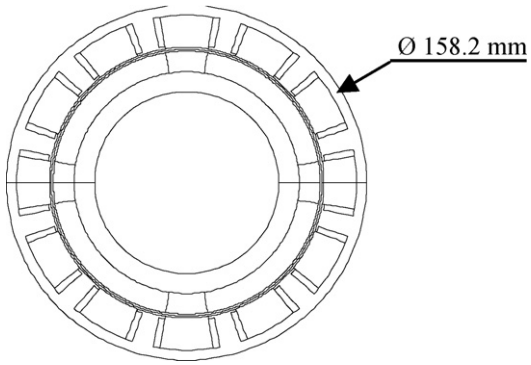

Fig. 22. PMSM for the system optimized by simultaneous optimization.

The greediness of the system optimized simultaneously comes from the ratio between the energy consumption and the performance to form the objective function. Thus by modifying this ratio, different systems could have been obtained (less or more dynamic, less or more powerful).

For the dynamic set point, the parameters given by PSO generate the engine profile and the control surface of Figs. 22 and 23.

These control laws and engine give us a response in mass flow with a very small smearing errors (maximal interval of 0.4788 g) and a consumption of 9133 J for this cycle of 60 s. The response is shown in Fig. 24.

Thus, with a simultaneous optimization, we obtain a system much more economic than the sequentially optimized system and on enormously more economic than the reference system. The counterpart is that the motor obtained by sequential optimization is double sized versus the reference one and that the machine obtained by simultaneous optimization is still a little bigger than the last one (Table 1). Ultimately, the previous results prove the effectiveness of the simultaneous optimization method using the particular swarms.

4.3. Coupled optimization with mass/energy criterion

Previous optimizations allow seeing PSO sizing capacity and improvement ability by system approach. But to obtain a realistic and useful structure of PMSM, it is necessary to adapt the optimization criterion. When we optimize only on an energetic

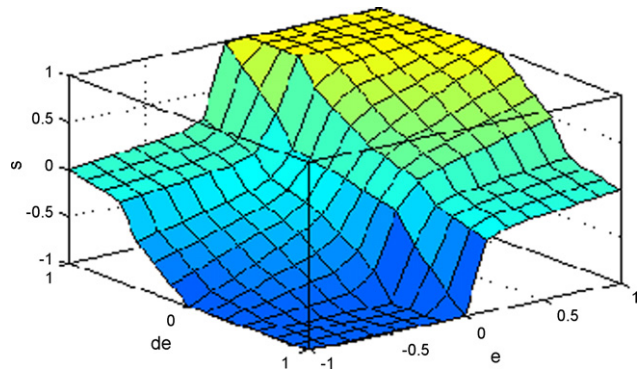

Fig. 23. Control law surface for the system optimized by simultaneous optimization.

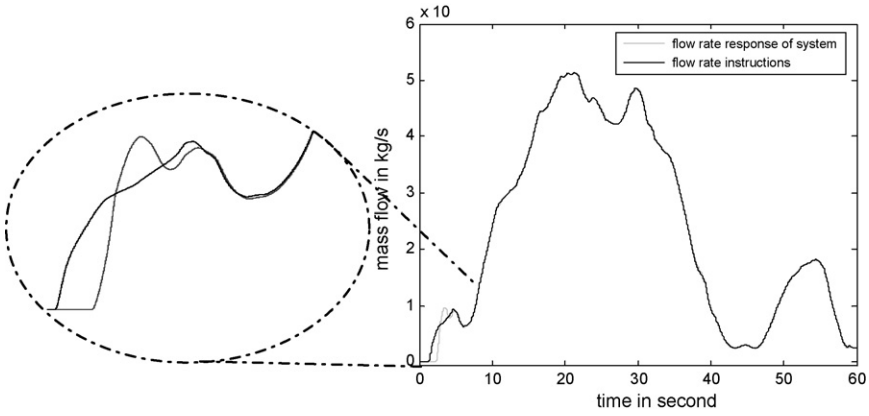

Fig. 24. Response in air mass flow at the dynamic set point.

Table 1
Summary table of the optimized system characteristics

Characteristic size	Initial system	System optimized sequentially for a dynamic solicitation and an energy criterion	System optimized simultaneously for a dynamic solicitation and an energy criterion	System optimized simultaneously for a dynamic solicitation and a mass/energy criterion
External radius	61.6 mm	79.1 mm	70.4 mm	75.7 mm
Motor length	30 mm	49.2 mm	73.9 mm	16.05 mm
Pole pair	2	2	2	6
Energy consumption	45,129 J	9,718 J	9,133 J	10,886 J
Motor mass	3.39 kg	6.94 kg	8.72 kg	1.07 kg

criterion, the algorithm tends to increase motor length to minimize energy consumption. But it is not always acceptable. It is, thus, more interesting to take an optimization criterion which is a compromise between energetic consumption and mass of PMSM. Optimization on 401 iterations with 20 particles in a unique swarm with a mass/energy criterion allows obtaining one new system. Fig. 25 shows PMSM structure and Fig. 26 shows fuzzy logic control law surface. This new system has an answer (Fig. 27) for the dynamic solicitation with a maximal smearing error of 4.34e-5 g and a consumption of 10,886 J on the cycle of 60 s. This system has more important energy consumption that both systems previously optimized but the energy motor is

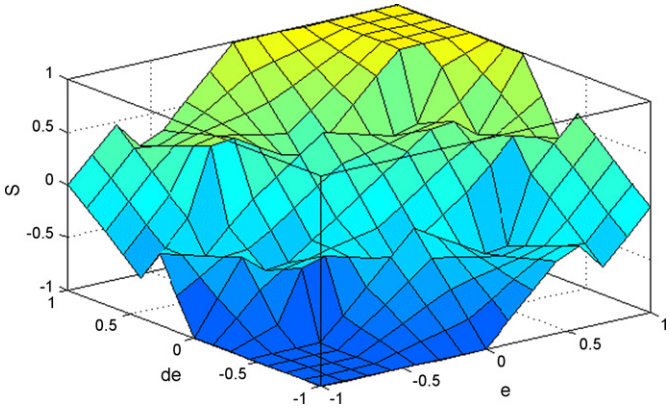

Fig. 26. Control law surface for the system optimized by simultaneous optimization with a mass/energy criterion.

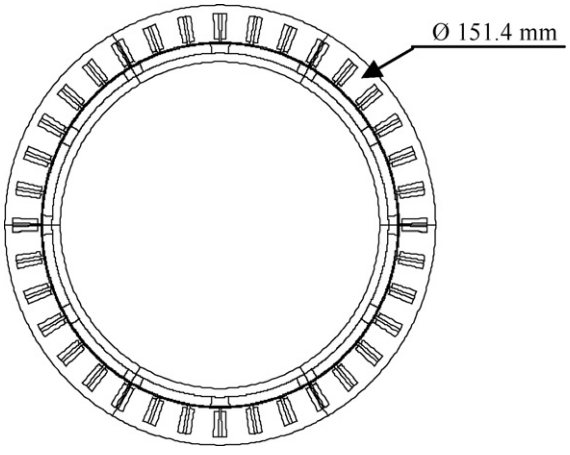

Fig. 25. PMSM for the system optimized by simultaneous optimization with a mass/energy criterion.

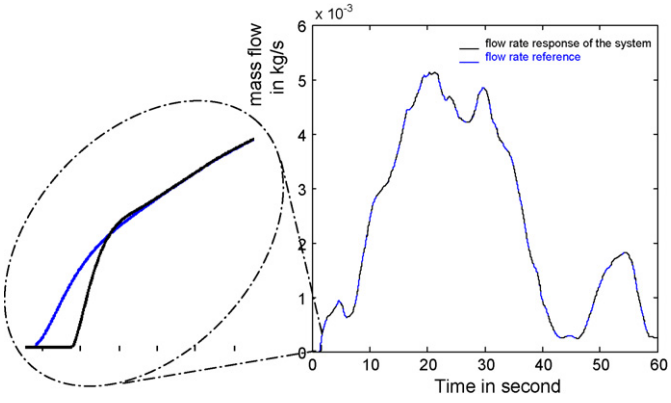

Fig. 27. Response in air mass flow for the dynamic set point for the system optimized by simultaneous optimization with a mass/energy criterion.

smaller. Table 1 compares obtained system characteristics. It is sharply visible that for about 20% more important energy consumption, motor mass is divided by 8. For an embedded system, this mass gain is very consequent.

5. Conclusion

In this paper, an innovating optimization approach for the design of a FC motor-compressor group shows its effectiveness based on the results obtained for various design tests. This method, known as simultaneous design, uses a system approach in order to design the whole system. This method combined with a heuristics such as PSO, shows its effectiveness in terms of implementation simplicity and required computing time. The different results proved that simultaneous optimization gives better results on this system than the sequential approach. However this approach must be validated on experimentation in real time. Moreover, it is presumable to still improve our results by including the parameters of the compression head model in the simultaneous optimization. Indeed, it will give a greater degree of freedom to the optimization program in order to achieve our goal to minimize the power consumption of the motor-compressor on a given mission cycle. Improvement could also be made into the analytical model of PMSM by taking into account excess losses such as iron or mechanical losses. This work is on progress in our laboratory.

References

[1] J. Milliken, F. Joseck, M. Wang, E. Yuzugullu, J. Power Sources 172 (1) (2007) 121–131.
[2] M. Tekin, D. Hissel, M.C. Pera, J.M. Kauffmann, J. Power Sources 156 (1) (2006) 57–63.
[3] C. Bao, M. Ouyang, B. Yi, J. Power Sources 156 (2) (2006) 232–243.
[4] F. Dubas, Conception d'un moteur rapide à aimants permanents pour l'entraînement de compresseurs de piles à combustible, Ph.D. Dissertation, University of Franche-Comté (UFC), Belfort, France, 2006.
[5] S. Vaez-Zadeh, A.R. Ghasemi, Electr. Power Syst. Res. 74 (2) (2005) 307–313 (available online at www.sciencedirect.com).
[6] J.-S. Chun (Seoul Natl Univ), J.-P. Lim, H.-K. Jung, J.-S. Yoon, IEEE Trans. Energy Conver. 14 (3) (1999) 610–615.
[7] M.A.P. Ramos, C.D.G. Beltran, J.T. Jimenez, Proceedings of the 2000 IEEE International Symposium on Industrial Electronics, ISIE 2000, vol. 2, December 4–8, 2000, pp. 741–746.
[8] J.O. Schumacher, P. Gemmar, M. Denne, M. Zedda, M. Stueber, J. Power Sources 129 (2) (2004) 143–151.
[9] A.S. Elwer, S.A. Wahsh, M.O. Khalil, A.M. Nur-Eldeen, The 29th Annual Conference of the IEEE, vol. 2, Industrial Electronics Society, IECON'03, November 2–6, 2003, pp. 1762–1766.
[10] H. Hu, Q. Hu, L. Lu, D. Xu, 32nd Annual Conference of IEEE, Industrial Electronics Society, IECON 2005, November 6–10, 2005, 5 pp.
[11] K. Fu, D. Sun, J.K. Mills, Proceedings of the 2002 IEEE International Symposium on Intelligent Control, 2002, pp. 746–751.
[12] H. Ando, K. Hiramoto, G. Obinata, Proceedings of the 41st SICE Annual Conference, vol. 1, SICE 2002, August 5–7, 2002, pp. 605–606.
[13] W. Na, B. Gou, J. Power Sources 166 (2) (2007) 411–418.
[14] S. Pischinger, C. Schönfelder, J. Ogrzewalla, J. Power Sources 154 (2) (2006) 420–427.
[15] D. Hissel, P. Maussion, J. Faucher, Eur. Phys. J. AP 16 (2001) 195–208.
[16] T. Markel, A. Brooker, T. Hendricks, V. Johnson, K. Kelly, B. Kramer, M. O'Keefe, S. Sprik, K. Wipke, J. Power Sources 110 (2) (2002) 255–266.
[17] M. Tekin, D. Hissel, M.-C. Pera, J.M. Kauffmann, IEEE Trans. Ind. Electron. 54 (1) (2007) 595–603.
[18] R.C. Eberhart, P. Simpson, R. Dobbins, Computational Intelligence PC Tools, Academic, New York, 1996.
[19] J. Kennedy, R.C. Eberhart, Proceedings of the IEEE International Conference on Neural Networks Perth, vol. IV, Australia, 1995, pp. 1942–1948.
[20] P.N. Suganthan, Proceedings of the IEEE International Congress on Evolutionary Computation, vol. 3, Department of Computer Science and Electrical Engineering, 1999, pp. 1958–1962.
[21] M. Clerc, J. Kennedy, IEEE Trans. Evol. Comput. 6 (2002) 58–73.
[22] K.E. Parsopoulus, M.N. Vrahatis, Proceedings of the Euro-International Symposium on Computational Intelligence, 2002.
[23] T. Ray, K.M. Liew, Proceedings of IEEE Congress on Evolutionary Computation (CEC 2001), Seoul, Korea, 2001, pp. 75–80.